The Developmental Morphospace of Wildfire

Ty Tuff, Ph.D.[1]

[1]Environmental Data Science Innovation & Impact Lab (ESIIL), Cooperative Institute for Research in Environmental Sciences (CIRES), University of Colorado Boulder, Boulder, Colorado, USA.

ORCID: 0000-0001-5249-5197

Correspondence: ty.tuff@colorado.edu

One-Sentence Summary

Fire VASE turns observed wildfire growth histories into standardized morphology, making developmental pathways a comparable response for mechanistic study.

Abstract

Most wildfire analyses compare events by endpoint summaries such as final area, duration, or peak growth. We introduce Fire VASE, which treats the ordered accumulation of burned area as morphology and converts observed developmental histories into normalized, comparable shapes. Across 278,569 FIRED events, histories varied continuously in when growth occurred, how long it persisted, and whether it accumulated steadily, pulsed, reactivated, or tapered. We then used centroid gridMET weather for 237,235 events as a first external explanatory layer. Centroid weather organized the distribution of developmental forms but did not uniquely specify individual histories. The fitted association between vapor pressure deficit and subsequent observed growth also depended on current fire state and was strongest when a fire was already growing rapidly. Weather–morphology mismatches identified fires for which the present environmental representation left substantial developmental variation unresolved. Fire VASE changes the response being explained: it provides a population-scale framework for studying how fires develop, not only how they end.

1 Introduction

A wildfire's final perimeter is the endpoint of a process. It records how much land burned, but not whether that area accumulated in one rapid run, through weeks of steady expansion, after a long delay, or in repeated episodes of growth and quiescence. Two fires can end at similar sizes after similar durations and still have little else in common. For communities, responders, and ecosystems, those different routes to the endpoint are often the consequential part of the event.

Recent work underscores the importance of growth itself. Across the United States, fast fires—defined as those growing more than 16.2 km^2 in one day—made up 2.7% of analyzed events but accounted for 88% of residential structures destroyed from 2001 to 2020 [1]. Yet the quantities commonly used to compare fires—final area, duration, severity, and mean or peak growth—still reduce the intervening sequence to one or a few numbers. They tell us that growth occurred, but not how it was organized through time.

Climate is an obvious candidate for organizing that sequence. Large-fire activity in western U.S. forests increased with warmer springs and summers and earlier spring snowmelt [2], and attribution studies have linked anthropogenic warming to increased fuel aridity and forest-fire area in the western United States and California [3, 4]. These studies establish strong climatic control over fire activity at regional and seasonal scales. They do not, by themselves, tell us why one individual fire grows early and stops, another persists, and another waits before making its largest run. Addressing that question requires a response variable that retains the history.

Fire science has long recognized that much of an event's expansion can be concentrated in particular spread episodes, and weather-based definitions of spread-event days have been used to improve fire-growth modeling [5]. Comparisons of unusually large and smaller fires further show that growth responses can differ even when differences in daily weather are modest [6]. More recent analyses using FIRED observations have related daily growth of individual western U.S. forest fires to aridity and prior fire size [7]. These studies motivate retaining the sequence of growth, but they do not provide a common normalized geometry for comparing the complete observed histories of many fires.

Here we treat fire development as morphology. Fire VASE places relative developmental time on a common vertical axis and normalized cumulative burned area on a radial axis. Each observed developmental slice adds a ring; the mapped area increment determines how far the form widens. The result is both a visual object and a quantitative trajectory that preserves the timing, persistence, concentration, and recurrence of observed growth. The approach follows the general logic of morphometrics for quantifying form, functional data analysis for comparing trajectories, and principal component analysis for identifying dominant axes of variation [8, 9, 10]. The contribution is not the drawing alone. It is the creation of a common response geometry in which whole developmental histories can be compared.

Satellite-based approaches already reconstruct daily fire progression [11], track individual fires globally to derive size, duration, daily expansion, speed, and spread direction [12], and use subdaily observations to update perimeters and active fronts [13]. Such data reveal strong regional differences in fire duration and spread [14]. Fire VASE complements these spatial and event-metric approaches by turning the complete observed sequence into a normalized geometry. We constructed the current representation from 278,569 MODIS-derived FIRED events comprising 626,102 observed developmental slices from 2000 to 2021 [15, 16, 17]. We then projected gridMET weather at the event centroid onto this fire-derived space for 237,235 climate-complete events [18].

We use the resulting space to ask a sequence of questions. Do observed histories vary along recurring developmental gradients? Does weather shift where fires occur in that space? Does current fire state alter the association between weather and subsequent observed growth? And what can be learned from cases in which weather and morphology disagree? Weather is the first demonstration of a broader explanatory architecture. Fire VASE makes developmental history the common response against which active-edge exposure, fuels, terrain, ignition context, suppression, and spatial progression can subsequently be tested.

2 Results

2.1 Observed growth histories become morphology

Figure 1 shows the transformation from an ordered burned-area record to morphology. Relative developmental time runs upward, each horizontal ring marks an observed developmental slice, and normalized width tracks the square root of the fraction of final observed area accumulated. Abrupt widening records a large mapped addition of area; nearly parallel sides record successive observations with little additional mapped growth; changes in slope record successive episodes of expansion. Read from bottom to top, a VASE is a compressed history of how the fire accumulated area.

The four observed fires make the encoding legible. A 1053.3 km^2 fire gains almost all of its normalized width in one early burst and then plateaus. A 3.2 km^2 fire widens gradually, producing a smooth funnel. An 11.4 km^2 fire remains narrow until a late surge, whereas a 19.5 km^2 fire records many alternating observations of expansion and relative quiet. Absolute area and recorded duration remain available as event attributes, but neither substitutes for these differences in sequence.

The VASE is not a geographic silhouette: width describes accumulated area, not perimeter shape or direction of travel. It is a standardized history. That distinction allows fires of very different sizes and durations to be compared without erasing when their growth occurred.

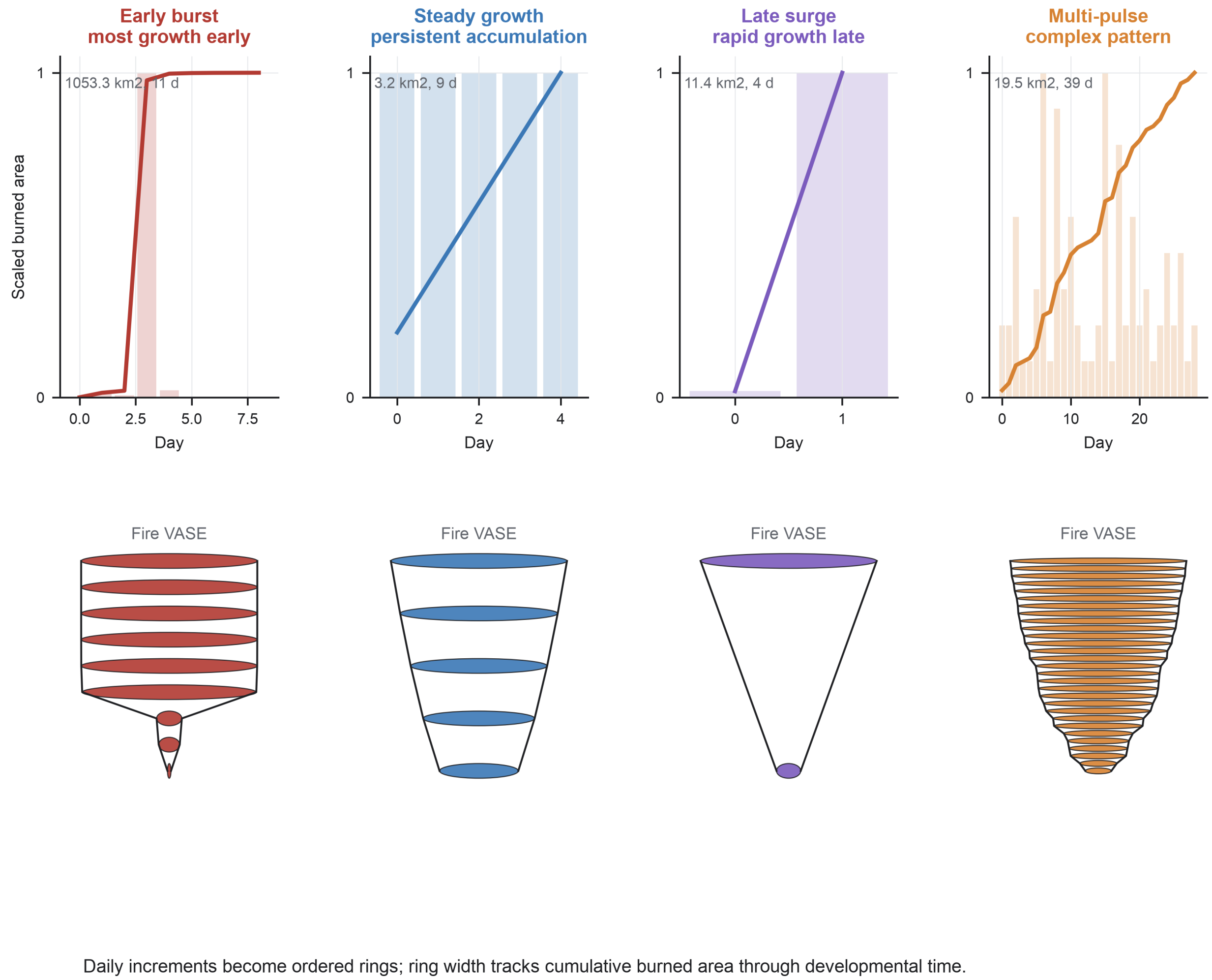

Figure 1: **Observed growth histories become morphology.** Four FIRED events illustrate information lost from final burned area and recorded duration. Upper panels show mapped burned-area increments as bars and cumulative burned area as lines, scaled within each fire and ordered by observation. Lower panels encode the same records as VASEs: relative developmental time runs upward, each ring represents an observed developmental slice, and normalized width tracks the square root of the fraction of final observed area accumulated. An early burst produces abrupt widening followed by nearly parallel sides; steady accumulation produces a smooth funnel; a late surge widens near the top; and repeated growth episodes produce an irregular profile with many rings.

2.2 Wildfire development varies along continuous gradients

Placed in a common coordinate system, the histories form a dense wedge rather than isolated clusters (Fig. 2A). VASE axis 1 primarily distinguishes concentrated, front-loaded growth from more distributed accumulation; axis 2 distinguishes when growth occurs and how long it persists within the observed record. Fires do not occupy isolated categories. They grade through combinations of timing, concentration, persistence, and recurrence.

Named neighborhoods make the main directions of variation interpretable without turning them into a taxonomy. Late-surge and front-loaded histories occupy opposing timing directions. Skinny-persistent and compact-steady forms both widen gradually but differ in how growth is concentrated through the observed record. The neighborhood labeled multi-pulse complex occupies a broad region associated with longer or more episodic records. Their overlap matters: many fires combine these behaviors, and the continuous coordinates preserve mixtures that a discrete classification would discard.

Occupancy of the space is highly uneven (Fig. 2B). Nearly 60% of events lie in the single-flash neighborhood and roughly 14% are skinny persistent; no other neighborhood contains 10% of events. A one-slice event contains no within-event trajectory, so single-flash occupancy reflects the observing system as well as fire behavior. Such records may represent genuinely brief burning, limits of MODIS observation, FIRED event-delineation rules, or some combination [15, 16]. The important result is the continuous organization of the observed histories; its stability among progressively better-observed fires remains the key immediate robustness test.

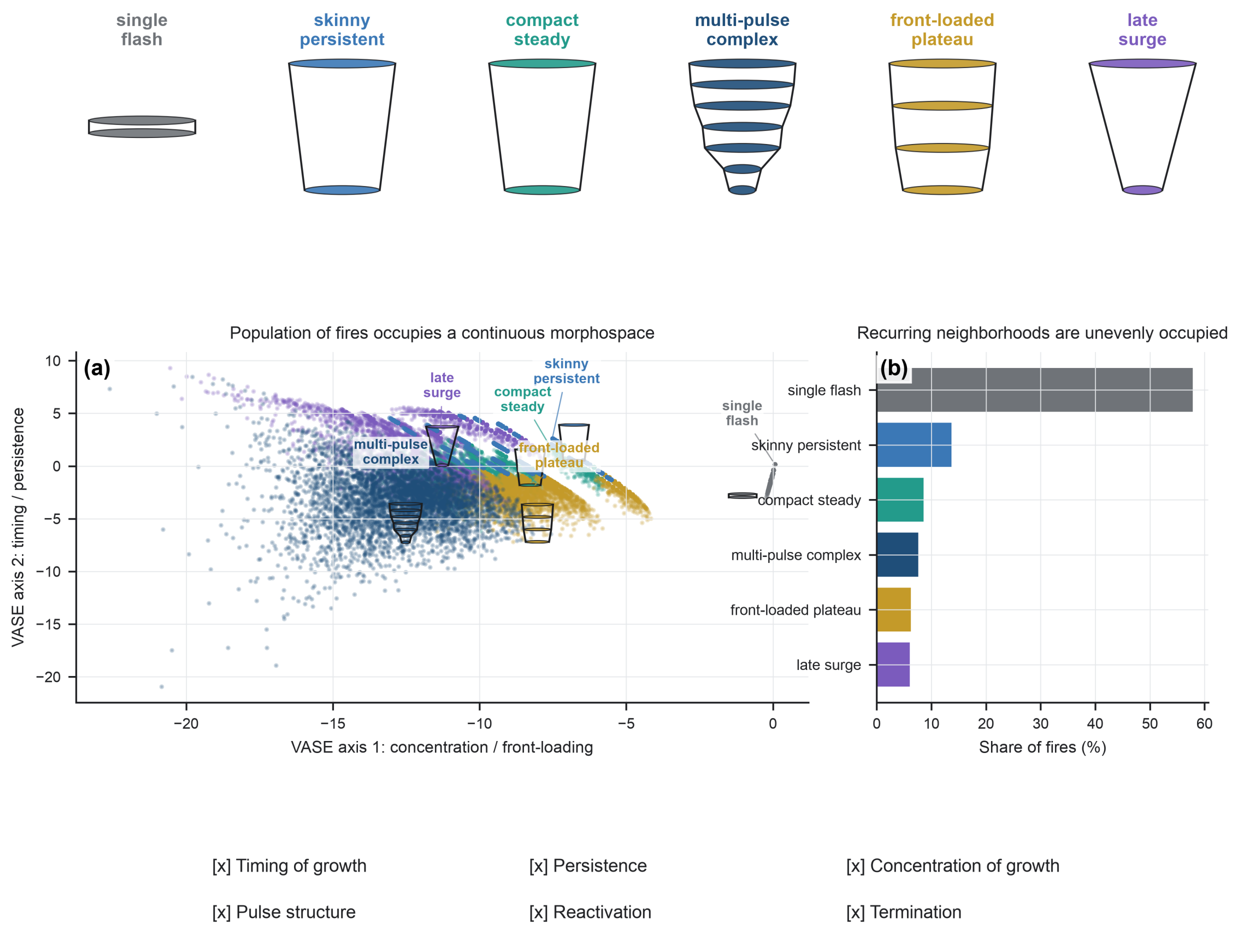

Figure 2: **Wildfire development varies along continuous gradients.** (A) Each point is one fire placed by the first two VASE axes. Axis 1 primarily describes concentration and front-loading, whereas axis 2 describes timing and persistence. Representative glyphs locate six descriptive neighborhoods, but the dense connecting cloud shows that intermediate and mixed forms are common. (B) Neighborhood occupancy is highly uneven: single-flash events constitute nearly 60% of fires, skinny-persistent histories roughly 14%, and each remaining neighborhood less than 10%. Single-flash events contain no internal developmental trajectory and are shown as an observationally important subset rather than a fire type.

2.3 Weather organizes but does not specify developmental form

Weather organized the morphospace without partitioning it. The maps in Fig. 3A–D show diffuse population-level gradients in maximum temperature, VPD, 1000-hour fuel moisture, and wind, but no sharp boundary separating one morphology from another. Environmental conditions shift where fires occur in developmental space without defining a unique form.

The VPD comparison makes this distributional association visible (Fig. 3E). Low-VPD fires contain more single-flash events; middle-VPD fires contain more skinny-persistent histories; and compact-steady and multi-pulse-labeled forms are modestly more common in the middle- and high-VPD groups. These differences are only a few percentage points, and every displayed neighborhood occurs in every tercile. Weather shifts the mixture of forms rather than assigning a characteristic VASE to each exposure group.

Individual weather dimensions align with different components of development (Fig. 3F). Higher event-mean precipitation is associated with less front-loaded growth, more late growth, greater entropy, and more pulses and reactivations. High-VPD and dry-fuel-slice fractions show weaker contrasts for several of the same responses, while mean temperature, humidity, and fuel moisture correlate only weakly with many shape-normalized traits. By changing the response, these comparisons distinguish associations with when growth occurs, how evenly it is distributed, and whether it appears to restart.

The predictive comparison reaches the same conclusion at the event level (Fig. 3G). The predictor set labeled core event means achieved median held-out $R^2 = 0.349$ across the developmental responses in the existing blocked analysis, leaving substantial variation among individual fires unresolved. Together, the prevalence, correlation, and prediction results show that centroid weather organizes the distribution of forms but does not uniquely identify an individual history.

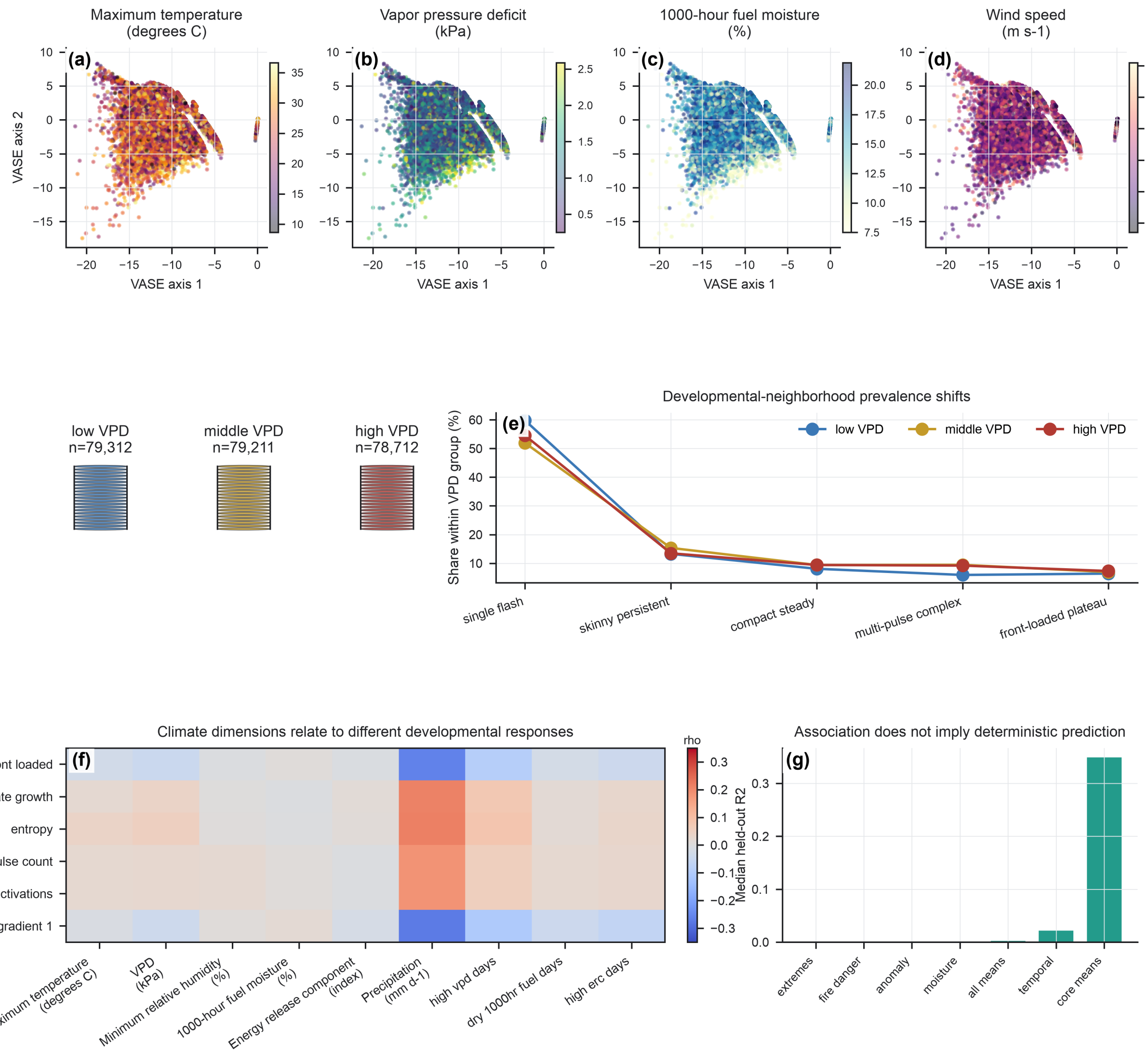

Figure 3: **Centroid weather maps onto developmental morphology without defining unique forms.** (A–D) Event-mean maximum temperature, VPD, 1000-hour fuel moisture, and wind produce diffuse gradients across the current morphospace. (E) VPD terciles differ modestly in neighborhood prevalence, but every neighborhood occurs in every tercile. (F) Weather summaries relate differently to the timing, evenness, pulsing, and reactivation of observed growth. (G) Blocked predictive models leave substantial variation among individual histories unresolved. The primary result is distributional: weather shifts where fires occur in developmental space without uniquely specifying their form.

2.4 Weather associations depend on current fire state

The morphospace treats development as more than an outcome; it also suggests that environmental exposure should be interpreted relative to a fire's current state. In the example histories above Fig. 4, relatively high within-fire VPD occurs before, during, and after rapid expansion. The same relative exposure can therefore accompany different positions in an observed developmental sequence.

Models of growth in the subsequent observed slice show the importance of that context (Fig. 4A). Weather alone explains roughly 0.03 to 0.09 of held-out variation. Current-sequence variables—developmental index, current growth, cumulative area, and acceleration—raise held-out R^2 to approximately 0.31–0.33 across validation schemes. This gain is expected to contain a strong autoregressive component. Adding weather yields smaller gains, and weather–state interactions reach about 0.35. The scientifically distinctive result is therefore not that recent growth predicts later growth, but that the fitted weather association differs across current fire states.

The fitted interaction with VPD illustrates that result (Fig. 4B). When current growth is low, fitted subsequent growth changes little across the displayed VPD range. When current growth is high, the fitted response rises from about 1.0 to 1.8 on the $\log(1 + \text{km}^2)$ scale as VPD increases from roughly 0.3 to 3 kPa. The same environmental exposure therefore has a different fitted association depending on the developmental state in which it occurs. This state dependence is associational rather than causal.

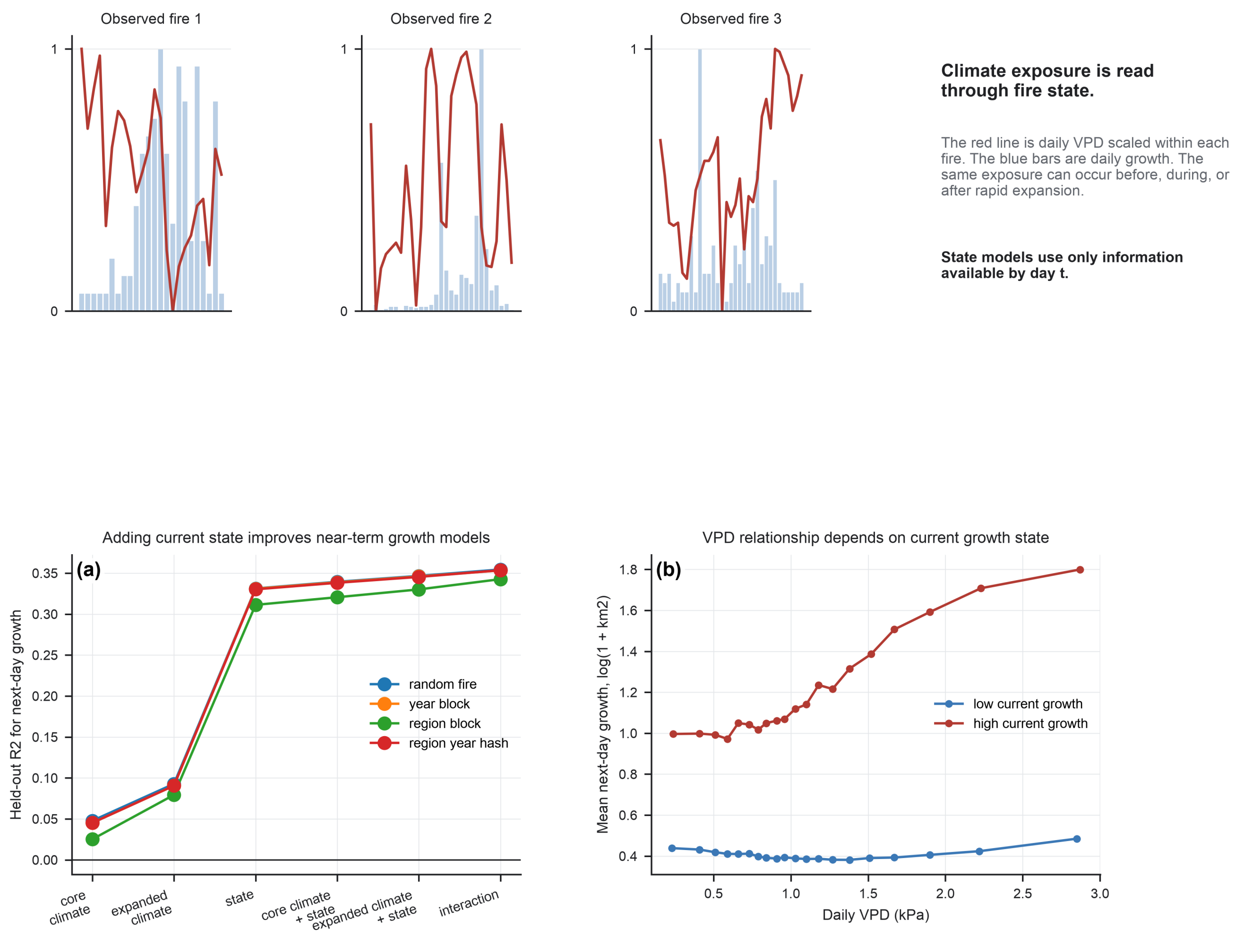

Figure 4: **The association between VPD and subsequent observed growth depends on current fire state.** The upper examples show that high VPD can occur at different positions in an observed growth sequence. (A) Autoregressive state variables explain substantially more held-out variation than weather alone; weather–state interactions provide additional information. (B) The fitted VPD association is nearly flat when current growth is low but positive when current growth is high. The result is an associational state dependence, not a causal estimate of VPD control.

2.5 Mismatches turn unexplained variation into testable cases

Figure 5 turns unexplained variation into candidate paired comparisons. Some fires with similar event-mean centroid weather follow sharply different developmental paths; conversely, similar developmental forms can occur under contrasting weather summaries. Across the sampled comparisons, weather-neighbor and morphology-neighbor searches produce different distance distributions (Fig. 5A). Similarity in one representation therefore does not guarantee similarity in the other.

The validation comparison reaches a related boundary from another direction (Fig. 5B). Current centroid-weather models explain only part of the variation in the developmental responses. The residual and mismatch cases are therefore candidates for testing where the present environmental representation, morphospace construction, or observation process is insufficient.

Those mismatches are scientifically useful because they identify fires for which additional explanatory layers may matter. Candidate explanations include fuel continuity, topographic confinement, ignition position, wind direction, suppression, conditions at the active edge, exposure error, observation error, and event delineation. Previous work shows that human ignitions expand the spatial and seasonal fire niche [19], environmental context shapes fire suitability [20], weather, fuels, and topography contribute to fire boundaries [21], and topographic controls on spread can be scale dependent [22]. Fire VASE provides a common response against which these alternatives can be tested; the present diagnostic examples do not identify which mechanism is responsible or estimate mismatch prevalence.

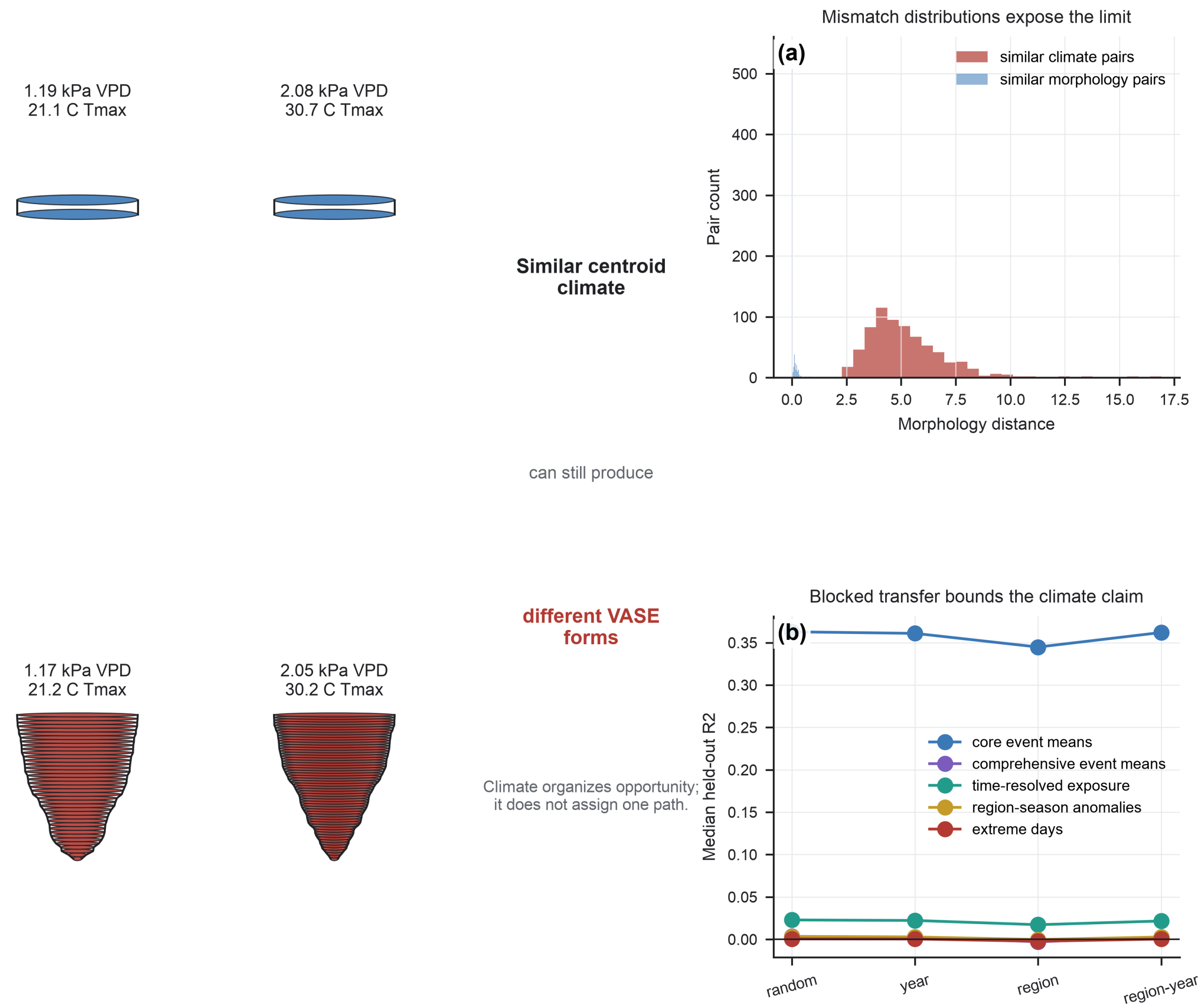

Figure 5: **Weather and developmental morphology have a many-to-many relationship.** Similar centroid weather can accompany contrasting developmental forms, and similar forms can occur under contrasting weather summaries. (A) Weather-neighbor and morphology-neighbor searches quantify these diagnostic mismatches. (B) Existing blocked models leave substantial developmental variation unresolved. The mismatches identify candidate fires for testing additional environmental, spatial, and observational explanations; they do not identify a mechanism or estimate its prevalence.

3 Discussion

Fire VASE changes the response being explained. Final area, duration, and peak growth remain important event attributes, but none substitutes for the sequence by which a fire developed. The normalized VASE makes early bursts, persistent expansion, late runs, pulsing, reactivation, and taper directly comparable as observed histories. Its principal contribution is this common developmental response geometry.

That geometry establishes an extensible program for fire science. Weather can be projected onto developmental morphology, followed by progressively more process-specific layers: conditions at the active edge, fuel continuity, terrain, ignition context, suppression, and the spatial geometry of progression. Each layer can be evaluated against the same response rather than against a different endpoint statistic. The present centroid-weather analysis is the first demonstration of this architecture, not its final application.

Within the current construction, observed histories form a continuum rather than a catalogue of fire types. The named neighborhoods anchor recognizable regions, but intermediate and mixed forms are common. A fire may be both persistent and episodic, or front-loaded with later reactivation. Continuous coordinates retain those combinations and make them available for comparison across events.

Weather's clearest pattern is distributional. Centroid conditions shift the prevalence of developmental forms without dividing the morphospace into distinct environmental regimes. Higher event-mean precipitation, for example, accompanies more late growth, greater entropy, and more pulsing and reactivation. These patterns do not identify a single mechanism: precipitation might separate growth into episodes, or longer fires may simply have more opportunity to encounter it. The value of the developmental response is that it reveals the temporal pattern the next analysis must explain.

The state models add a second lesson. The fitted association between weather and subsequent observed growth differs with current fire state. High VPD has little fitted association when current growth is low but a stronger positive association when current growth is high. This interaction is more informative than the expected autoregressive result that current growth predicts later growth.

It suggests that environmental exposure should be interpreted conditional on system state, while remaining an associational rather than causal result.

The weather–morphology mismatches extend the framework from description to hypothesis generation. Fires that are close in weather space but distant in developmental space, or vice versa, identify cases in which the current explanation is insufficient. Fuel continuity, topographic confinement, ignition context, suppression, active-edge geometry, exposure error, observation error, and event delineation are competing explanations. Fire VASE does not distinguish among them, but it identifies the fires in which they can be tested.

Several limitations define the present scope. Many events contain only one observed slice, and adjacency in the ordered record has not been confirmed as uninterrupted calendar time. The current PCA combines normalized developmental features with absolute event attributes and is therefore weather-independent but not endpoint-independent. Final-event-centroid weather is retrospective and cannot represent conditions along a moving active edge. Weather associations may retain geographic, seasonal, and year structure; state variables contain strong autoregressive information; predictor-set comparisons require additional auditing; and the selected mismatch examples do not estimate prevalence. The multi-observation and shape-only sensitivities are therefore the two immediate tests of whether the developmental gradients persist beyond the current construction.

Even within these boundaries, the representational advance is clear. Fire VASE turns the developmental history itself into a standardized response. It allows fire science to ask not only which conditions accompany large or long fires, but why fires accumulate area through different developmental pathways.

4 Materials and Methods

The analysis proceeded in four stages. We first converted each ordered FIRED burned-area record into a normalized VASE history. We then described variation among histories with developmental traits and a multivariate morphospace. Next, we projected centroid weather onto that fire-derived coordinate system. Finally, we evaluated event-level weather associations, state-dependent subsequent growth, and selected cases in which weather similarity and developmental similarity diverged.

4.1 Fire observations and ordered developmental histories

Fire histories were derived from FIRED event and observation products for the conterminous United States and Alaska, which delineate events from the MODIS burned-area product [15, 16, 17]. For each event, the source data identify the fire, its ignition and final dates, recorded duration, final mapped area, and final event geometry. Associated observations provide a date, an event-day field, newly mapped burned area, and cumulative mapped burned area.

Within each fire, observations were ordered by date and event-day field. Adjacency in this ordered sequence denotes adjacency in the available observation record; it has not been established that every adjacent pair represents consecutive calendar days. We therefore refer to the rows as observed developmental slices rather than assuming an uninterrupted daily time series. Negative mapped-area increments were set to zero, and cumulative observed area was calculated as the cumulative sum of the resulting nonnegative increments. The analysis contains 278,569 events and 626,102 observed slices spanning 2 November 2000 through 1 May 2021.

4.2 Converting an observed history into a VASE

Each fire was represented by the way its observed burned area accumulated through relative developmental time. For a fire with more than one slice, the ordered sequence was scaled from 0 at its first observation to 1 at its last observation. One-slice fires were placed at the midpoint of this relative-time scale. This transformation aligns histories of different recorded lengths by their position within the observed sequence; it does not assert equal elapsed time between slices.

For each observed slice, ring area was the nonnegative increment in mapped burned area. Cumulative observed area determined the width of the VASE. For a positive-area fire, normalized VASE width at developmental time t was defined as

$$w(t) = \sqrt{\frac{A(t)}{A(T)}}, \tag{1}$$

where $A(t)$ is cumulative observed burned area at developmental time t and $A(T)$ is final cumulative observed burned area. Every positive-area VASE therefore terminates at normalized width 1. Up to a constant, $w(t)$ is proportional to the radius of an equal-area disk; the square-root transformation converts relative area to a radius-like dimension. Abrupt widening indicates that a large fraction of final observed area was added in one part of the sequence, whereas nearly parallel sides indicate successive observations with little additional mapped growth. Absolute burned area is not represented directly by normalized VASE width, although absolute event attributes are included in the current multivariate morphospace.

4.3 Developmental feature construction

We described each observed history with scalar summaries and interpolated profiles. Scalar developmental summaries measured the timing, concentration, evenness, and recurrence of growth. They included the relative position of maximum observed growth; the fractions of area accumulated in the first and final portions of the sequence; the amount of growth remaining at the final observation relative to the observed maximum; the number of major-growth episodes and subsequent reactivations; the evenness of area allocation among slices; and the average magnitude of changes in VASE width. The current feature set also includes recorded final area, duration, observation count, slenderness, and a fire-trait growth summary labeled peak growth. It therefore combines normalized developmental form with absolute event attributes.

Major-growth episodes were identified within each fire. A slice belonged to a major-growth episode when its mapped-area increment exceeded the greater of the within-fire 75th percentile, 25% of maximum observed growth, and a small positive floor. Pulse count was the number of transitions into such episodes; reactivation count was pulse count minus one, bounded below by zero. Front-loaded growth was the fraction of final observed area accumulated by relative developmental time 0.5. Late growth was the fraction added after relative time 0.75, and terminal taper was final-slice growth divided by maximum observed slice growth.

Growth entropy measured how evenly positive growth was allocated among observed slices and was normalized by the logarithm of the number of slices [23]. Developmental velocity and acceleration were the mean absolute first and second differences of normalized VASE width across the ordered sequence. Because these measures treat adjacent observations as adjacent developmental positions, interpretations involving persistence, reactivation, velocity, or acceleration depend on the spacing of observation dates.

To retain more of the trajectory than scalar summaries alone, normalized width and growth were also linearly interpolated to 11 common positions in relative developmental time. The resulting profiles describe how cumulative form and incremental growth change from the beginning to the end of an observed history.

4.4 Current multivariate morphospace and descriptive neighborhoods

The current Fire VASE morphospace was fitted from these fire-derived event attributes, developmental summaries, and interpolated profiles without using weather predictors. Before principal component analysis [10], final area, duration, the growth summary labeled peak growth, and slenderness were log-transformed. Missing values were replaced with the median of the corresponding feature, and every feature was centered and scaled to unit variance. Principal components were then computed by singular value decomposition, and the first five scores were retained as continuous coordinates of developmental variation.

Weather variables were attached only after this coordinate system was defined. The PCA is therefore weather-independent but not endpoint-independent: final area, duration, and related absolute-scale variables contribute to the current axes alongside normalized developmental traits and profiles.

For interpretation, fires were also assigned to descriptive neighborhoods using observation count, duration, final area, pulse count, peak timing, front-loaded fraction, terminal taper, and population quantiles. One-slice events were labeled single flash; the remaining labels were skinny persistent, multi-pulse complex, late surge, front-loaded plateau, and compact steady. These labels are landmarks rather than statistically inferred classes. Prevalence summaries use the labels, whereas model analyses use continuous traits and morphospace coordinates.

4.5 Projecting weather onto developmental histories

After the fire-derived morphospace was constructed, we associated each observed fire date with gridMET weather [18]. For each event, the final mapped geometry was projected to an equal-area coordinate system, its centroid was calculated, and that location was transformed back to longitude and latitude. Weather for every observed date was taken from the nearest gridMET cell to the fixed event centroid. The resulting exposure is retrospective: it represents weather at the centroid of the completed event rather than conditions at a contemporaneous active edge.

The attributed variables were maximum and minimum temperature, VPD, wind speed, precipitation, maximum and minimum relative humidity, specific humidity, 100-hour and 1000-hour fuel moisture, energy release component, burning index, reference and potential evapotranspiration, and solar radiation. Maximum and minimum temperature were converted from Kelvin to degrees Celsius. An observed slice was considered weather-complete only when every requested variable was available. Complete centroid-weather histories were obtained for 237,235 fires. Spatial summaries based on event perimeters, newly and cumulatively burned area, and perimeter extension were developed as supplemental exposure products but were not used for the main population analysis.

4.6 Weather summaries and developmental response variables

For each weather-complete fire, we summarized conditions across the observed history using the mean, observed minimum, observed maximum, and means within the early, middle, and late thirds of relative developmental time. We also calculated a region–month anomaly by subtracting the median value among fires observed in the same broad region and calendar month. This anomaly is a contrast within the fire population, not a departure from an independent climatological normal.

To represent episodic exposure, we calculated the fraction of observed slices exceeding population-wide thresholds. Hot, high-VPD, windy, and high-ERC slices exceeded the 90th percentile of the corresponding fire-slice distribution; dry 1000-hour fuel-moisture slices fell below its 10th percentile; wet slices had precipitation greater than zero.

The event-level responses were selected to distinguish absolute outcomes from developmental form.

They included front-loaded fraction, late-growth fraction, terminal taper, growth entropy, pulse count, reactivation count, peak timing, recorded duration, final area, and the first morphospace coordinate. Duration, area, pulse count, and reactivation count were transformed as $\log(1 + x)$ before model fitting.

We used these responses in two complementary ways. Correlations described how individual weather summaries aligned with different components of observed development. Predictive models then asked how well groups of centroid-weather summaries transferred to fires held out in time, space, or both. These analyses measure population association and predictive transfer; they do not isolate causal weather effects from geography, season, year, or unmeasured fire conditions.

4.7 Event-level weather models and validation

Event-level predictive models used ridge-regularized linear regression with penalty $\alpha = 1.0$. Predictor groups were designed to test progressively different representations of centroid weather: core atmospheric conditions, moisture and humidity, fire-danger and energy variables, combined event summaries, region–season anomalies, extreme-slice fractions, and weather resolved across early, middle, and late development. The current core group contains event-mean maximum temperature, minimum temperature, VPD, and wind speed together with available summaries of maximum VPD. Because an observed maximum and an event mean respond differently to record length, comparisons among predictor groups are interpreted as descriptive baselines rather than definitive rankings of weather representations.

The moisture group contained precipitation, relative and specific humidity, and 100-hour and 1000-hour fuel moisture. The fire-danger and energy group contained energy release component, burning index, reference and potential evapotranspiration, and solar radiation. The time-resolved group combined early-, middle-, and late-development summaries with extreme-slice fractions.

All predictors were standardized using only the training portion of each validation fold and then transformed with the same training estimates in the held-out portion. Random-fire folds provided a diagnostic of interpolation among similar observations. More conservative tests held out broad year blocks, broad geographic regions, or hashed region–year combinations.

For each response and fold definition, held-out R^2 compared predictions with the mean of the held-out response after fold predictions were concatenated. The manuscript's blocked summary combines the year, region, and region–year tests rather than the random-fire diagnostic. These tests evaluate transfer under the implemented blocking definitions; they do not by themselves estimate a weather effect independent of geographic or seasonal structure.

4.8 State-dependent subsequent-growth models

The state-dependent analysis asked whether the association between weather at an observed slice and growth at the subsequent observed slice varied with the fire's current condition. Within each weather-complete fire, the mapped-area increment from the next retained slice was shifted backward to serve as the response for the current slice and transformed as $\log[1 + \text{area (km}^2)]$. This construction requires another retained observation and is therefore conditional on continuation in the model table. A next-calendar-day interpretation additionally requires confirmation that adjacent retained slices are separated by exactly one day.

Current fire state was represented by position in the observed developmental sequence, current mapped growth, cumulative observed area, and the change in mapped growth from the previous slice. Growth and cumulative area were transformed as $\log[1 + \text{area (km}^2)]$. Final duration, final area fraction, future growth, and VASE coordinates were not used as explicit state predictors. Weather nevertheless came from the centroid of final event geometry, so the complete model is retrospective rather than an operational forecast using only contemporaneously available fire locations.

We compared weather-only, state-only, additive weather-plus-state, and weather–state interaction models. Interaction terms paired each core weather variable with developmental position, current growth, and current cumulative area. Estimation, within-fold standardization, and validation followed the event-level procedure. Because state variables are strongly autoregressive, the principal scientific contrast is the incremental association of weather and weather–state interactions beyond the state-only baseline.

These models estimate conditional associations, not causal weather effects. Current and subsequent growth may share unmeasured causes, and interpretation of the displayed VPD-by-state relationship depends on uncertainty and empirical support across that domain.

4.9 Composite histories and mismatch comparisons

Individual VASE glyphs display the observed history of one fire. To summarize groups without averaging events of different observed lengths directly, each normalized width profile was interpolated to 41 common positions in relative developmental time. Composite VASEs show the median width at each position together with the interquartile range. Weather-conditioned composites divide weather-complete fires into low, middle, and high terciles of event-mean centroid VPD.

Representative fires were selected deterministically using fixed seeds and prespecified scoring rules. Mismatch comparisons standardized the selected centroid-weather variables and morphospace coordinates so that distances were measured in comparable units. The examples were chosen to illustrate that proximity in weather space need not imply proximity in developmental space, and vice versa. They are diagnostic examples rather than estimates of mismatch prevalence; their interpretation depends on the current morphospace, observation-count distribution, distance definitions, and matching rules.

4.10 Reproducibility and scope of inference

The analysis was organized as a versioned sequence from source observations through derived histories, statistical summaries, and figures. Input and output manifests record file identities and checksums; fixed seeds control sampling, validation folds, and representative-fire selection; and the main figures can be regenerated from the archived data package. Derived statistics are written before plotting so that numerical claims can be checked independently of figure rendering.

The present scope is constrained by both the fire observations and the environmental representation. Final-event-centroid weather does not capture within-perimeter heterogeneity, active-edge conditions, directional wind exposure, gusts, fuels, vegetation, topography, suppression, ignition context, or independent local climate normals. Many fires have only one observed slice, and adjacency in the ordered sequence has not been shown here to equal uninterrupted calendar time. The current PCA also incorporates endpoint quantities alongside normalized developmental features. The analysis should therefore be read as a first projection of environmental information onto a multivariate representation of observed fire development, not as a complete, causal, or endpoint-independent explanation of fire-growth pathways.

References and Notes

References

[1] J. K. Balch *et al.*, The fastest-growing and most destructive fires in the US (2001 to 2020). *Science* **386**, 425–431 (2024). doi:10.1126/science.adk5737.

[2] A. L. Westerling, H. G. Hidalgo, D. R. Cayan, T. W. Swetnam, Warming and earlier spring increase western U.S. forest wildfire activity. *Science* **313**, 940–943 (2006). doi:10.1126/science.1128834.

[3] J. T. Abatzoglou, A. P. Williams, Impact of anthropogenic climate change on wildfire across western US forests. *Proc. Natl. Acad. Sci. U.S.A.* **113**, 11770–11775 (2016). doi:10.1073/pnas.1607171113.

[4] A. P. Williams, J. T. Abatzoglou, A. Gershunov, J. Guzman-Morales, D. A. Bishop, J. K. Balch, D. P. Lettenmaier, Observed impacts of anthropogenic climate change on wildfire in California. *Earth's Future* **7**, 892–910 (2019). doi:10.1029/2019EF001210.

[5] J. Podur, B. M. Wotton, Defining fire spread event days for fire-growth modelling. *Int. J. Wildland Fire* **20**, 497–507 (2011). doi:10.1071/WF09001.

[6] B. E. Potter, D. McEvoy, Weather factors associated with extremely large fires and fire growth days. *Earth Interact.* **25**, 160–176 (2021). doi:10.1175/EI-D-21-0008.1.

[7] C. S. Juang, A. P. Williams, J. T. Abatzoglou, J. K. Balch, M. D. Hurteau, M. A. Moritz, Rapid growth of large forest fires drives the exponential response of annual forest-fire area

to aridity in the western United States. *Geophys. Res. Lett.* **49**, e2021GL097131 (2022). doi:10.1029/2021GL097131.

[8] F. L. Bookstein, *Morphometric Tools for Landmark Data: Geometry and Biology* (Cambridge Univ. Press, 1991).

[9] J. O. Ramsay, B. W. Silverman, *Functional Data Analysis*, ed. 2 (Springer, 2005). doi:10.1007/b98888.

[10] I. T. Jolliffe, *Principal Component Analysis*, ed. 2 (Springer, 2002). doi:10.1007/b98835.

[11] S. Veraverbeke, F. Sedano, S. J. Hook, J. T. Randerson, Y. Jin, B. M. Rogers, Mapping the daily progression of large wildland fires using MODIS active fire data. *Int. J. Wildland Fire* **23**, 655–667 (2014). doi:10.1071/WF13015.

[12] N. Andela, D. C. Morton, L. Giglio, R. Paugam, Y. Chen, S. Hantson, G. R. van der Werf, J. T. Randerson, The Global Fire Atlas of individual fire size, duration, speed and direction. *Earth Syst. Sci. Data* **11**, 529–552 (2019). doi:10.5194/essd-11-529-2019.

[13] Y. Chen *et al.*, California wildfire spread derived using VIIRS satellite observations and an object-based tracking system. *Sci. Data* **9**, 249 (2022). doi:10.1038/s41597-022-01343-0.

[14] J. A. Balik, J. D. Coop, M. A. Krawchuk, C. E. Naficy, M.-A. Parisien, S. A. Parks, C. S. Stevens-Rumann, E. Whitman, Biogeographic patterns of daily wildfire spread and extremes across North America. *Front. For. Glob. Change* **7**, 1355361 (2024). doi:10.3389/ffgc.2024.1355361.

[15] L. Giglio, L. Boschetti, D. P. Roy, M. L. Humber, C. O. Justice, The Collection 6 MODIS burned area mapping algorithm and product. *Remote Sens. Environ.* **217**, 72–85 (2018). doi:10.1016/j.rse.2018.08.005.

[16] J. K. Balch, L. A. St. Denis, A. L. Mahood, N. P. Mietkiewicz, T. M. Williams, J. McGlinchy, M. C. Cook, FIRED (Fire Events Delineation): An open, flexible algorithm and database of US fire events derived from the MODIS burned area product (2001–2019). *Remote Sens.* **12**, 3498 (2020). doi:10.3390/rs12213498.

[17] A. L. Mahood, E. J. Lindrooth, M. C. Cook, J. K. Balch, Country-level fire perimeter datasets (2001–2021). *Sci. Data* **9**, 458 (2022). doi:10.1038/s41597-022-01572-3.

[18] J. T. Abatzoglou, Development of gridded surface meteorological data for ecological applications and modelling. *Int. J. Climatol.* **33**, 121–131 (2013). doi:10.1002/joc.3413.

[19] J. K. Balch *et al.*, Human-started wildfires expand the fire niche across the United States. *Proc. Natl. Acad. Sci. U.S.A.* **114**, 2946–2951 (2017). doi:10.1073/pnas.1617394114.

[20] M.-A. Parisien, M. A. Moritz, Environmental controls on the distribution of wildfire at multiple spatial scales. *Ecol. Monogr.* **79**, 127–154 (2009). doi:10.1890/07-1289.1.

[21] L. M. Holsinger, S. A. Parks, C. Miller, Weather, fuels, and topography impede wildland fire spread in western US landscapes. *For. Ecol. Manage.* **380**, 59–69 (2016). doi:10.1016/j.foreco.2016.08.035.

[22] N. A. Povak, P. F. Hessburg, R. B. Salter, Evidence for scale-dependent topographic controls on wildfire spread. *Ecosphere* **9**, e02443 (2018). doi:10.1002/ecs2.2443.

[23] C. E. Shannon, A mathematical theory of communication. *Bell Syst. Tech. J.* **27**, 379–423 (1948). doi:10.1002/j.1538-7305.1948.tb01338.x.

Acknowledgments

Funding: Funding information to be added before submission.

Author contributions: Author contributions to be completed before submission.

Competing interests: The authors declare no competing interests.

Data and materials availability: The external FIRED, MODIS burned-area, and gridMET inputs are publicly available from the cited sources. Derived analysis tables, figure-generation scripts, manuscript-generation code, and the shareable Fire VASE data-lake package are organized in the Fire VASE repository. Repository DOI, CyVerse accession, or archival accession to be added before submission.

AI transparency: OpenAI Codex/ChatGPT was used as an AI-assisted coding, analysis, visualization, and editorial tool during development of this project. AI assistance included drafting and revising Python scripts for Fire VASE data ingestion, climate attribution, morphospace analysis, statistical summaries, figure generation, PDF/report production, and render-based quality checks; drafting and revising manuscript text, figure legends, response-to-review material, and simulated reviewer critiques; searching for and organizing candidate citations and author-guideline requirements; and helping maintain logs, manifests, tests, schemas, and documentation.

The AI system did not originate the underlying FIRED, MODIS burned-area, gridMET, PRISM, or other observational data, did not make final scientific judgments independently, and is not listed as an author. Human investigators directed the analyses, selected the scientific claims, reviewed code and outputs, verified calculations and citations where reported, and remain responsible for the integrity, interpretation, and final content of the manuscript.

Synthetic or illustrative demonstrations created during repository development are documented separately and were not used as evidentiary data for the manuscript analyses.

Supplementary Materials

Supplementary Methods S1 to S10, Supplementary Results S11 to S15, Figs. S1 to S4, and Tables S1 to S7 are provided in a separate Supplementary Materials document.